Journal of The Electrochemical Society, **150** (8) A1030-A1036 (2003)
0013-4651/2003/150(8)/A1030/7/$7.00 © The Electrochemical Society, Inc.

Electrochemical Studies of Nickel and Copper/Yttria Titania Zirconia Ceria Cermets

J. C. Ruiz-Morales,[a,b] Pedro Núnez,[a,z] Richard Buchanan,[b] and John T. S. Irvine[b,*]

[a]*Departamento de Química Inorgánica, Universidad de La Laguna, Tenerife, Canary Islands, Spain*
[b]*School of Chemistry, University of St. Andrews, Scotland, United Kingdom*

The aim of this work was to investigate the electrochemical performance of yttria-zirconia-titania-ceria ($Y_{0.15}Zr_{0.57}Ti_{0.13}Ce_{0.15}O_{1.925}$) and its metal composites in hydrocarbon fuels. The materials were prepared by the ceramic method, and characterized by X-ray diffraction (XRD) thermogravimetry and dilatometry. DC conductivity measurements, at 900°C, were performed as a function of p_{O_2}. The electrochemical performance on its own or as cermets with nickel or copper was investigated using a two-electrode, symmetrical cell format. Experiments were performed in air, 5% H_2 (wet) and 5% CH_4 (wet) to investigate the electrochemical processes, utilizing the AC impedance spectroscopy technique in the temperature range 500-900°C. The material is found to retain its cubic fluorite structure on reduction despite all the Ce^{4+} being reduced to Ce^{3+}. The thermal expansion coefficient is close to that of yttria-stabilized zirconia (YSZ) and the conductivity is largely dominated by oxide ionic, with a small electronic contribution. The copper-based cermets perform well at 600°C, but microstructural degradation due to Cu migration decreases performance at higher temperatures. Surprisingly the electrode performance in air, for CuO/YZTC6, is reasonable. Overall, however, problems with Cu migration indicate that this composite is only an interesting anode for low temperature use (<600°C). Nickel-based cermets did not show such good performance at low temperatures; however, their performance was the best at higher temperatures, but still an order of magnitude lower than Ni/YSZ cermets with optimized microstructure.
 [DOI: 10.1149/1.1584437]

Manuscript received September 30, 2002. Available electronically June 16, 2003.

Solid oxide fuel cells (SOFCs) are a very promising technology for power generation, because SOFCs are thermodynamically more efficient than competing heat-engine power plants and with lower emissions of NO_x, CO_2, and unreacted hydrocarbons than other conventional generators.[1] Many researchers have investigated the electrode reaction to improve the cell performance. Since hydrogen, methane, methanol, etc. are used as fuel for SOFCs it is important to understand in detail the electrode reaction on the anode side.

A major objective is the development of SOFC anodes capable of operating in natural gas, without suffering from carbon build up due to catalytic cracking; this objective is still far from being achieved. The cermets of the nickel/yttria stabilized zirconia (Ni/YSZ) are the most commonly used anode material, since they are inexpensive and exhibit high catalytic activity for hydrogen oxidation.[2] Despite excellent properties for operation in hydrogen, the Ni-based electrode suffers from some disadvantages related to the volume instability upon redox cycling and detrimental carbon formation caused by the cracking of hydrocarbon reactants.[3] The rapid deposition of carbon at Ni cermets means that direct oxidation of methane is not technically viable in Ni-containing SOFCs. Cracking is even more problematic with higher hydrocarbons, which are also present in natural gas. For mixtures of CH_4 and H_2O, the catalytic properties of Ni cause steep thermal gradients over the first few millimetres from entry of the fuel gas into the cell. The endothermic nature of the steam reforming process can thus cause steep thermal gradients potentially capable of mechanically damaging the cell stack.[4]

The nickel loading is generally chosen to be slightly in excess of the limit for percolation electronic conduction.[5] At higher Ni loadings, there are problems with thermal expansivity mismatch between the Ni and the zirconia electrolyte substrate.[6]

In order to utilize natural gas as fuel in this type of SOFC, the fuel is usually externally or internally reformed with steam.[3] Internal reforming is attractive; however there are potential difficulties due to thermal gradients as reforming is endothermic and oxidation exothermic. External reforming is currently the method of choice; however there would be cost benefits and considerable scope for improved engineering design if the external reforming stage could be eliminated. Direct oxidation is a very attractive alternative and some important advances have been achieved utilizing ceria-containing anodes at temperatures of operation below that at which methane cracks.[7] Work is also underway to develop new materials that catalyze direct oxidation so that it can compete effectively with cracking at higher temperatures.

Underlying the electrochemical activity of an electrode material is the ability of charged species to migrate from the electrolyte to the surface and their availability at the surface to perform electrochemical reactions. If an electrode is able to transport both electrons and ions from electrolyte to the surface then it will allow electrochemical reactions to occur across the complete electrode surface, not just at three phase boundaries between electrode, electrolyte, and gas phase.[8] This affords much better activity and may be viewed as a catalytic effect. Zirconia-mixed conductors are good candidates to replace the state of the art in SOFC cermets anodes. Ceria- and titania-doped YSZ mixed conductors could be good candidates as the fuel electrode matrix.[9-20]

The importance of this mixed conductivity has recently been demonstrated in work at St Andrews focused upon titania-doped YSZ[21] showing that poor electronic conductivity can be compen-

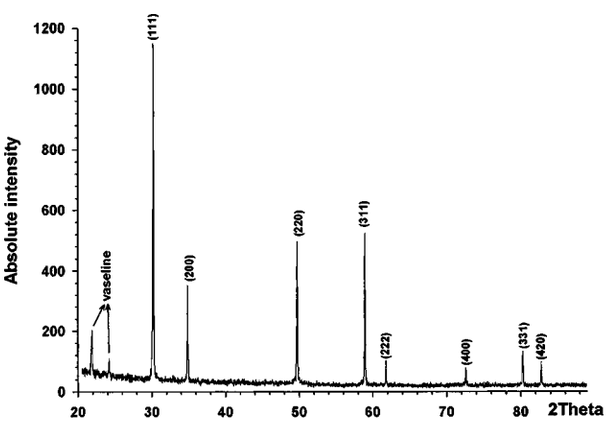

Figure 1. A typical X-ray diffractogram of $Y_{0.15}Zr_{0.57}Ti_{0.13}Ce_{0.15}O_{1.925}$ after firing in air, $a = 5.1673$ Å for the cubic fluorite.

* Electrochemical Society Active Member.
z E-mail: pnunez@ull.es

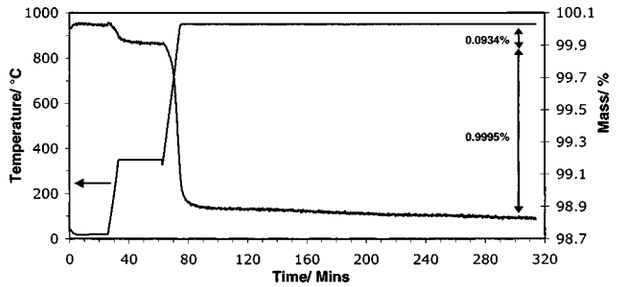

Figure 2. TGA of reduction of $Y_{0.15}Zr_{0.57}Ti_{0.13}Ce_{0.15}O_{1.925}$ under 5% H_2/argon. (Mass losses corrected for buoyancy).

sated by good ionic conduction. This material exhibits good compatibility with zirconia, excellent ionic conduction, but poor electronic conduction. Because electronic conduction is probably the most important consideration for a fuel cell electrode, this material has performed exceedingly well delivering power densities approaching 50 $mWcm^{-2}$.[22]

Electrochemical impedance spectroscopy (EIS) is one of the most used techniques in the investigations of various electrolyte and electrode/electrolyte interfacial processes.[23] With EIS the contributions of various electrode processes are separated in the frequency domain.

In this work we have combined the good properties of the titania-doped YSZ system with the good catalytic behavior of ceria ($Y_{0.15}Zr_{0.57}Ti_{0.13}Ce_{0.15}O_{1.925}$, YZTC6). The electrochemical properties of YZTC6 on its own in composites with NiO or CuO have been studied using EIS. From this data it is observed that YZTC6 is a mixed conductor under reducing conditions. We have also compared the properties of the traditional anode material (NiO composite) with the properties of CuO composite, given that copper is an excellent electronic conductor and inert to hydrocarbon activation.

Experimental and Results

Structural properties of YZTC6.—The $Y_{0.15}Zr_{0.57}Ti_{0.13}Ce_{0.15}O_{1.925}$ (YZTC6), sample 1, is a material taken from studies on the Y_2O_3-ZrO_2-TiO_2-CeO_2 system. It was prepared from solid-state reaction of Y_2O_3 (Alfa Aesar), ZrO_2 (Fluka), TiO_2 (Aldrich), and cerous nitrate (Alfa Aesar). These oxides were previously dried at 300°C and mixed in the appropriate ratios according to the formula to obtain about 20g of YZTC6, by heating at 1400°C for 96 h with intermittent grinding. The phase purity was checked by powder X-ray diffraction, showing a single phase of fluorite type with a unit cell of 5.167(1) Å, Fig. 1. Unit cell parameters were obtained using the transmission Stoe Stadi-P X-ray diffractometer (10-90° 2θ, step size 0.5° 2θ, Cu Kα1 radiation).

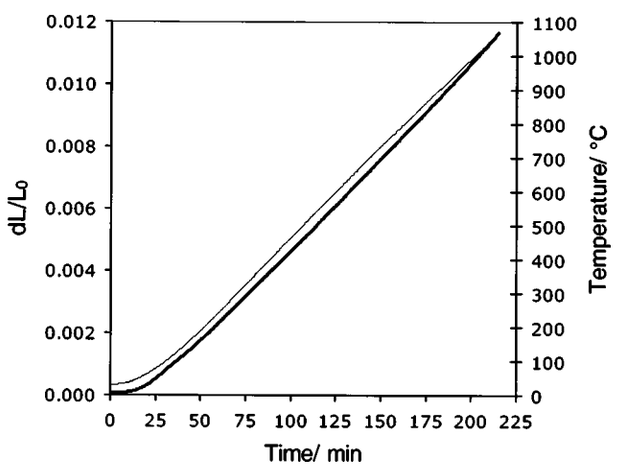

Figure 3. Thermal expansion of YZTC6 measured in oxygen. (Thin line = temperature.)

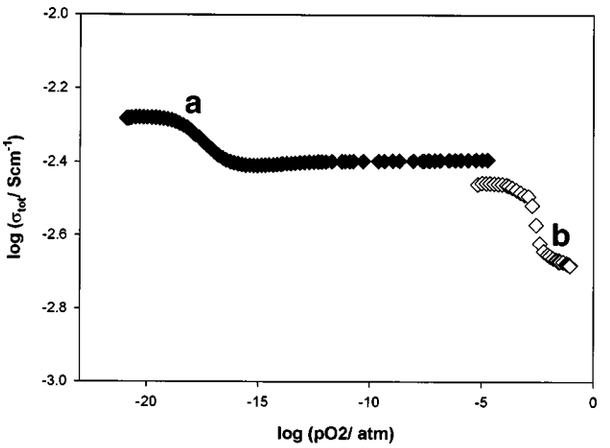

Figure 4. Dependence of electrical conductivity upon partial pressure of O_2, (a) closed symbols measured on slow oxidation after equilibration in 5% H_2/95% Ar and (b) open symbols on slow oxidation from Ar.

Thermogravimetric analysis (TGA) of YZTC6.—TGA measurements were performed by holding the temperature of the sample at 20°C for 15 min, followed by heating at 50°C min^{-1} to 350°C and a dwell of 30 min. Then heating again at 50°C min^{-1} to 950°C and a dwell of 240 min. The atmosphere used was 5% H_2/argon flowing at 20-30 cm^3min^{-1}. Studies were carried out on a Rheometric TGA2 1000M instrument. Figure 2 shows the TGA plot for the reduction of the YZTC6.

After accounting for buoyancy, the mass losses were 0.0934% at up to 350°C and 0.9995% from 350-950°C. The first mass loss (up to 350°C) was attributed to moisture and the second mass loss (350-950°C) was due to the reduction of the material. The mass loss of ~1% was in line with the prediction of how much mass would be lost if all of the cerium in the material were reduced from Ce^{4+} to Ce^{3+} (0.973%). X-ray diffraction (XRD) analysis of the reduced sample showed that the structure was still cubic, although the unit cell increased to 5.1854(7) Å, from 5.167(1) Å.

Tube furnace reduction of YZTC6.—Qualitative reduction involved heating up pellets of YZTC6 placed in an alumina boat in a horizontal tube furnace in 5% H_2/argon at 1000°C, with a piece of copper foil used as an oxygen scrubber. The first reduction run involved heating at 1000°C for 46 h in "wet" 5%H_2/argon (bubbled through water). The result was that the sample lost 0.88% of mass and changed color from light brown to dark brown/black. The unit cell expanded from 5.1673 to 5.1799 Å. The sample was reoxidized in oxygen at 1000°C for 48 h and the oxidized material was pale yellow, while the unit cell shrunk back to 5.1670 Å.

In the second reduction run, another pellet was reduced in 5% H_2/argon for 88 h. This time, the amount of mass lost was 1.00% and the unit cell expanded to 5.1828 Å. The appearance of the reduced sample was as for the first reduction run.

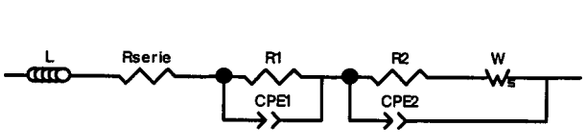

Scheme 1. Equivalent circuit used for data fitting. *L*: inductance element from the wires. R_{series}: include all ohmic losses. R-CPE elements: charge transfer processes. W_s: diffusion element.

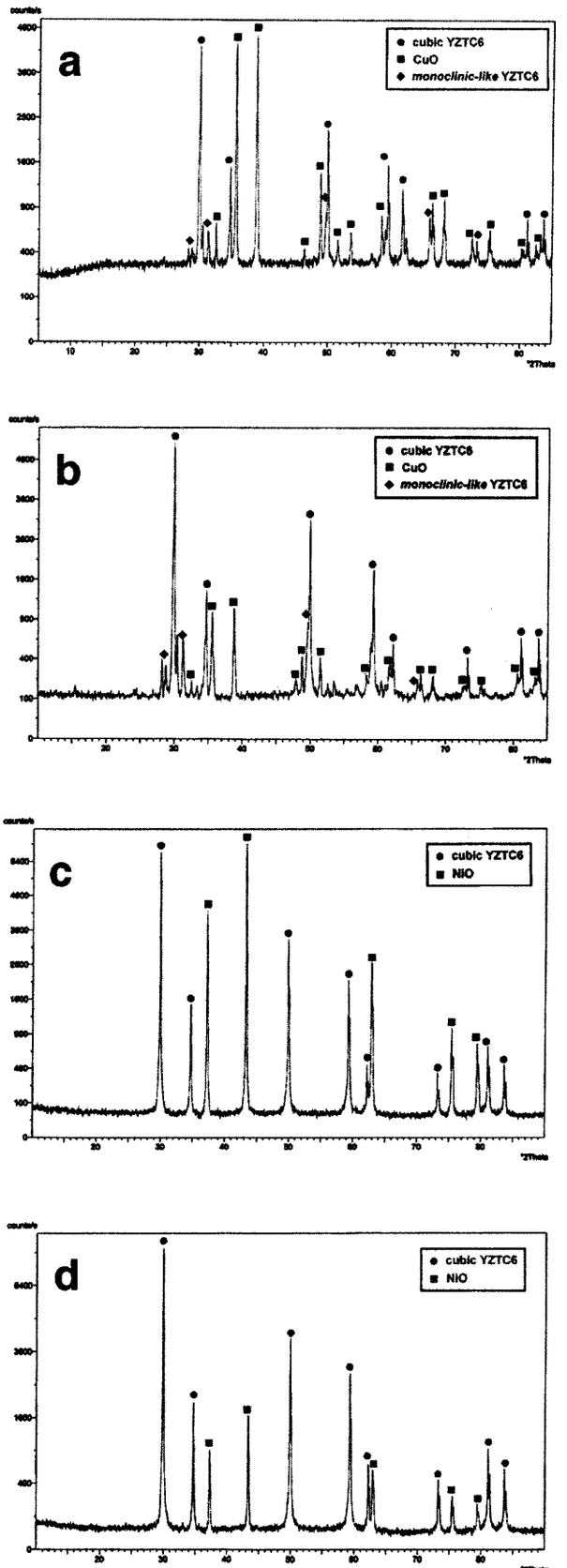

Figure 5. X-ray powder diffractogram of 40% w/w YZTC6-CuO (a), 80% w/w YZTC6-CuO (b), 40% w/w YZTC6-NiO (c), 80% w/w YZTC6-NiO (d), cermets in oxidized state.

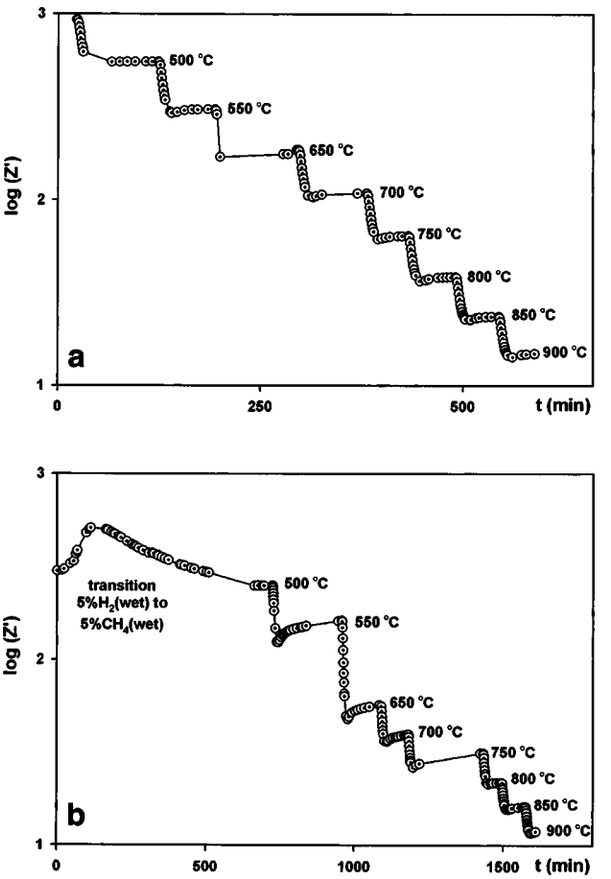

Figure 6. Reproducibility measurements, for (a) sample 1, ac perturbation 5 mV, $f = 1$ MHz, and (b) sample 2a, ac perturbation 5 mV, $f = 100$ kHz.

Thermal expansion coefficient (TEC) of YZTC6.—In determining the TEC (α) of the material, a pellet 9.219 mm thick was heated up in oxygen from ambient to 1100°C at 5°C min^{-1} and cooled at the same rate to ambient. Prior to that, a background measurement was taken using an alumina cylinder of similar size run under the same conditions, Fig. 3. α was measured between 200 and 1025°C to be 11.21×10^{-6} K^{-1}. This lies between α for YSZ ($\sim 10.3 \times 10^{-6}$ K^{-1}) and for CeO_2 (12.1×10^{-6} K^{-1}) in that temperature region.

DC conductivity studies of YZTC6.—DC conductivity studies involved isothermal measurements at 900°C, where conductivity was measured as a function of p_{O_2}, which was investigated using two separate experiments. The first one started from 5% H_2/argon and was slowly allowed to reoxidize, Fig. 4a, and the second starting from argon and again allowed to reoxidize with a slow air leak, Fig. 4b.

The fairly smooth changeover from the data obtained on starting from 5% hydrogen to that obtained starting from argon indicated that the intermediate $p_{(O_2)}$ conductivity values were fairly close to equilibrium. To a first approximation, conductivity was independent of oxygen partial pressure, with only small deviations from a value of 3×10^{-3} Scm^{-1} as partial pressure was varied. This would be consistent with dominant oxide ionic conductivity. Two regions show small decreases in conductivity as oxygen partial pressure was increased. The slopes associated with these regions are much smaller than $p_{(O_2)^{-1/6}}$ also indicative of dominant oxygen ion conductivity. The changes are thought to indicate two regions of decreasing electronic contribution to the overall conductivity.

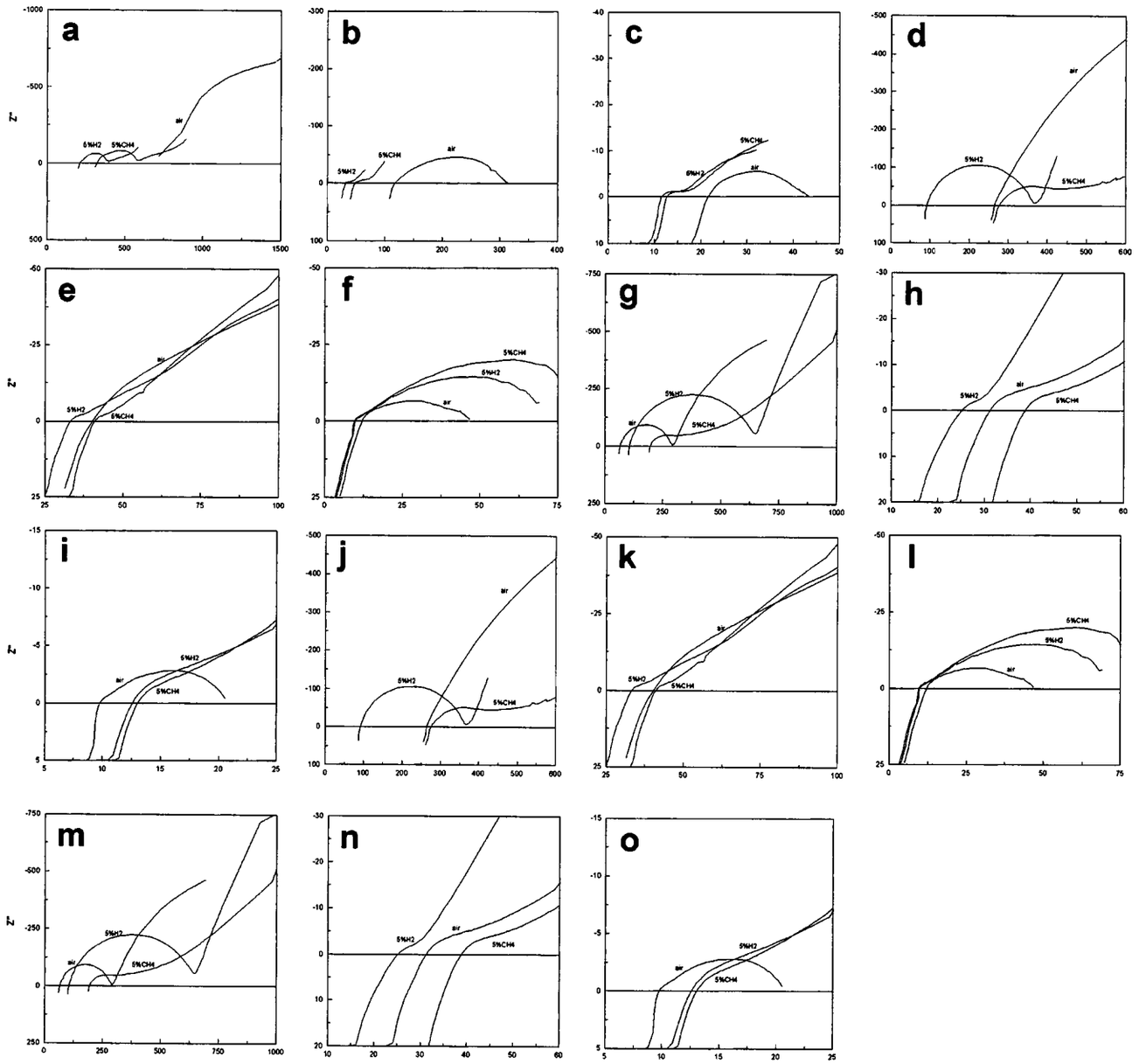

Figure 7. Symmetrical-cell measurements for: sample 1 (YZTC6) at (a) 500°C, (b) 700°C, (c) 900°C; sample 2a (YZTC6 + 20% CuO), at (d) 500°C, (e) 700°C, (f) 900°C; sample 2b (YZTC6 + 60% CuO), at (g) 500°C, (h) 700°C, (i) 900°C; sample 3a (YZTC6 + 20% NiO), at (j) 500°C, (k) 700°C, (l) 900°C; sample 3b (YZTC6 + 60% NiO), at (m) 500°C, (n) 700°C, (o) 900°C, in air, 5% H_2 (wet) and 5% CH_4 (wet).

Cermet preparation.—Four cermets have been prepared by mixing YZTC6 with NiO (Aldrich) and CuO (Aldrich) in different weight ratios (sample 2a, YZTC6:CuO = 40:60; sample 2b, YZTC6:CuO = 80:20; sample 3a, YZTC6:NiO = 40:60 and sample 3b, YZTC6:NiO = 80:20).

The NiO and CuO were previously dried at 500°C for 2 h. The powder mixtures for the cermets with the corresponding weight ratios were planetary ballmilled in acetone for 1 h using a zirconia container with zirconia balls. Then, the powders were fired at 1000°C, in air, for 24 h, and the purity was checked by powder XRD, Fig. 5. For NiO cermets, the peaks corresponding to reflections of NiO and YZTC6 are shown in Fig. 5c and d, but for CuO cermets new peaks, surrounding the major YZTC6 peaks, have been found, Fig. 5a and b. Probably, in the YZTC6-CuO system, tetragonal zirconia was formed due to reaction of CuO at 1000°C, and was fully converted to monoclinic zirconia on cooling and grinding, but the cubic was still the main phase.

Slurries of samples 1, 2a, 2b, 3a, and 3b were prepared, mixing with a binder (Decoflux VB41). These slurries were used to paint two identical and symmetrical layers on each side of YSZ-20%Al_2O_3 electrolyte plates from CeramTec AG (Germany).

Electrochemical studies of cermets.—The symmetrical cells with an anode of area 0.95 cm^2, and about 125 μm thickness of the electrodes were sintered onto the 300 μm thick electrolyte at 1200°C, in air, for sample 1 and 3, and 1000°C, in air, for sample 2. The electrode materials were coated with an organoplatinum paste on each face, dried at 100°C for 1 h and fired at 1000°C for 1 h.

The samples were mounted in a ''compression jig'' with Pt wire electrodes, in a horizontal tube furnace. Temperature dependent re-

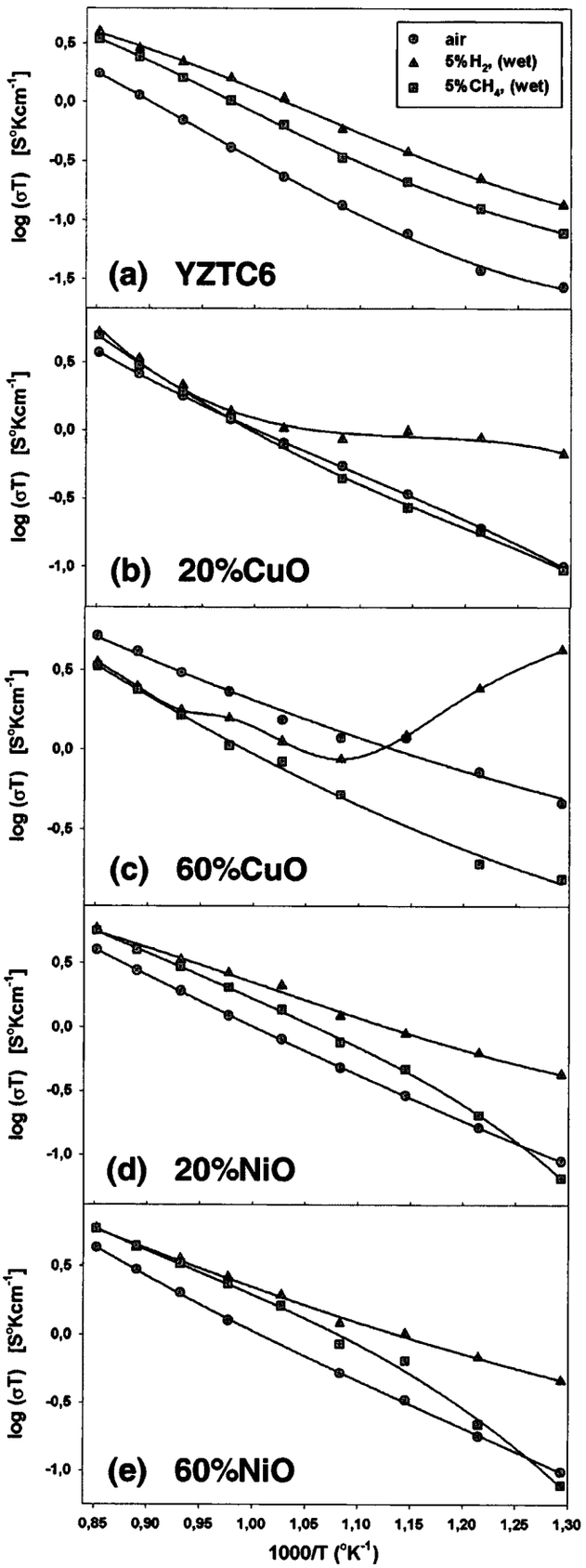

Figure 8. Temperature dependence of R_{series}, symmetrical cell: (a) YZTC6, (b) YZTC6 + 20% CuO, (c) YZTC6 + 60% CuO, (d) YZTC6 + 20% NiO, and (e) YZTC6 + 60% NiO, on heating.

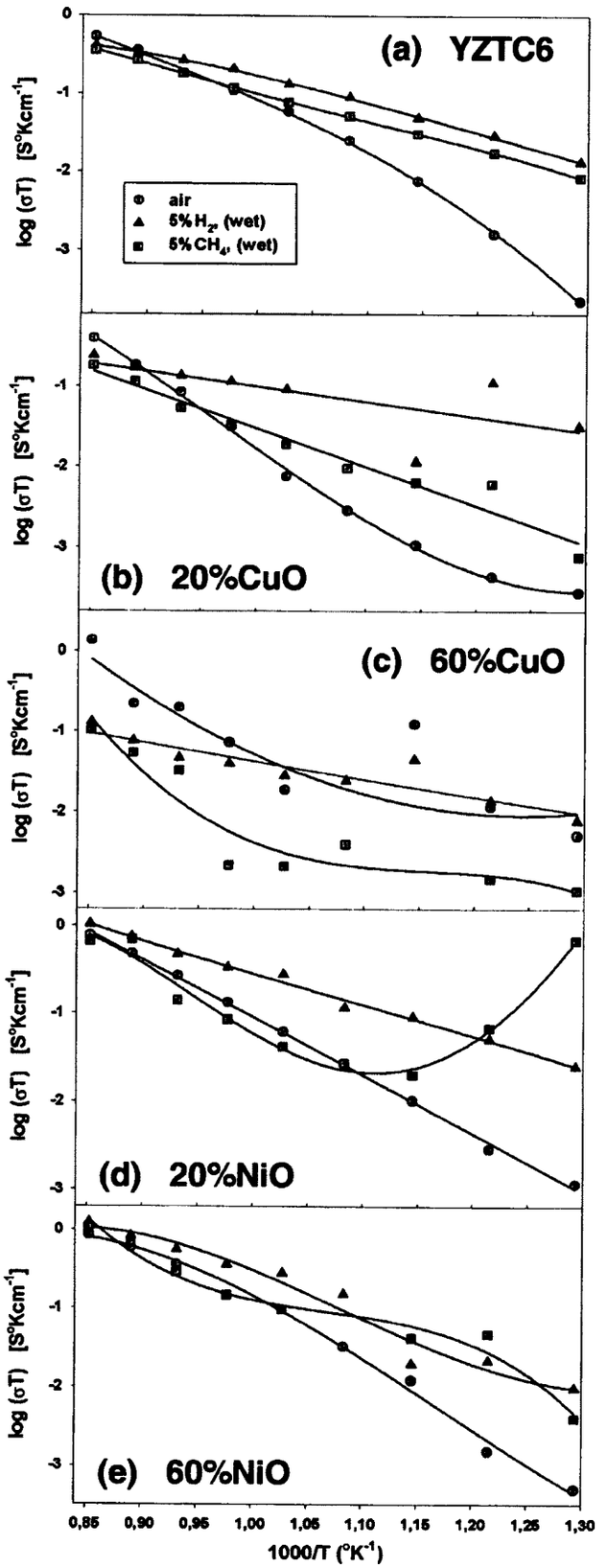

Figure 9. Temperature dependence of $R_{polarization + diffusion}$, symmetrical cell: (a) YZTC6, (b) YZTC6 + 20% CuO, (c) YZTC6 + 60% CuO, (d) YZTC6 + 20% NiO, and (e) YZTC6 + 60% NiO, on heating.

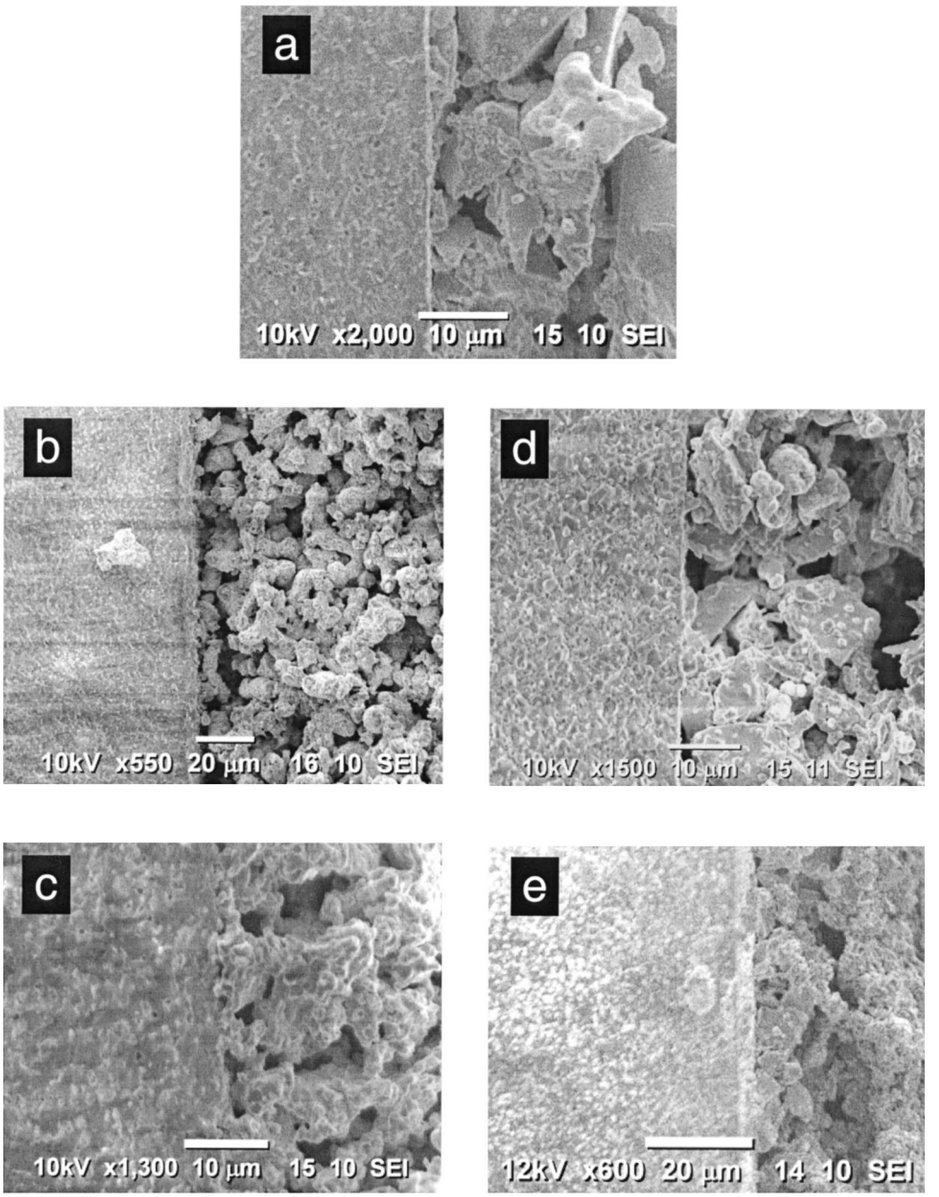

Figure 10. Cross-sectional SEM micrographs, (a) YZTC6, (b) YZTC6 + 20% CuO, (c) YZTC6 + 60% CuO, (d) YZTC6 + 20% NiO, and (e) YZTC6 + 60% NiO.

sistance corrections have previously been determined for the jig. Measurements were also corrected for lead inductance. The ac impedance measurements on symmetrical cells were performed sequentially in air, 5% hydrogen (wet) and 5% methane (wet) in 50°C steps between 500 and 900°C, cooling back to 500°C before changing atmosphere. For each temperature sufficient time was allowed to obtain thermal equilibrium and the reproducibility of the measurements. To achieve this, we monitored the sample, performing measurements at only one high frequency against the time, if there is no measurement artifact at high frequency, the value of Z' must correspond with the value of the series resistance R_s element. So plotting this value *vs.* time provided a tool to assess the reproducibility of the measurements, Fig. 6. From this plot, it was possible to point out that we need different waiting-times for each sample and for each gas composition, for example: for sample 1, in air, Fig. 6a, the waiting time is the same for each temperature, but for sample 2a, in methane, Fig. 6b, the waiting time can be as long as 3 h at 550°C, or just about 1 h at temperatures above 750°C.

The impedance measurements were performed with a Solartron 1260 frequency response analyser, at OCP, with a 15 mV of a.c. perturbation. Measurements were carried out in the 1 MHz to 0.1 Hz frequency domain. Typical ac impedance measurements for each sample are shown in Fig. 7, at three different temperatures and in three different gas compositions.

The impedance spectra generally showed a well-resolved single arc at low temperature. The high frequency intercept of this arc with the real axis corresponds to the series resistance of the electrolyte and electrode. The electrode can have two influences on this value, first, a direct contribution from the series resistance of the electrode itself and second, a reduction in effective contact area due to the poor lateral connectivity of the thin electrode layer. At higher temperature this arc is less well defined and becomes distorted at high frequencies due to the inductance of the measuring circuit. The arc, which has a capacitance of 1-10 μF, is related to the electrode polarization phenomena as are the additional low frequency arcs and diffusion features that may also be evident.

In all cases, both series and polarization resistances decreased at high temperature. These resistances were much smaller in reducing atmospheres. The performance in wet methane (5%) was very similar to that in wet hydrogen (5%), at higher temperatures. But the

performance was better in wet hydrogen (5%) at low temperature; however it should be noted that these measurements were carried out in sequence on the same samples. Thus part of the deterioration in performance in CH_4 at least can be attributed to events that occur on heating in H_2.

The impedance has been analyzed in terms of equivalent circuit theory. The best fitting to the curves such as those shown in Fig. 7, can be obtained with the following model: a combination of a series resistance and inductance element, at high frequencies; one or two R-constant phase elements (CPEs) at intermediate frequencies related with the charge transfer processes; and at lower frequencies a Warburg impedance from the gas diffusion. Analysis of the impedance data was performed with the computer program ZPLOT v2.2 from Scribner.

The value of these elements depends on both the material and the gas composition. The typical value for the inductance is approximately 1×10^{-5} H at lower temperature and 3×10^{-6} H at higher temperature. The exponent values of the CPE elements are usually between 0.75 and 0.85 at lower temperature. The exponents of the Warburg element were around 0.45.

In order to obtain the series, polarization and diffusion resistances of the materials, we used the equivalent circuit corresponding to Scheme 1.The Arrhenius plots for the series, polarization and diffusion contributions, shown in Fig. 8, 9 were obtained from the values determined from the fitting of the experimental data, correcting the data for the jig, electrolyte resistances and the geometrical factor.

For all the samples, the performance in hydrogen and methane was similar at higher temperature, above 850°C. For the samples with CuO, Fig. 8b and c, the best performance with regard to the series resistance was obtained with the sample of 60% CuO at 500°C, Fig. 8c, but this relative performance decreased with temperature with a transition around 650°C. Above this temperature the conductivity in hydrogen and in methane was similar, indicating that any difference between these conditions relates to changes in microstructure on initial heating to 650°C. There is probably a segregation of Cu from the anode material to the interface between the electrolyte and the anode material at this temperature, decreasing performance. Surprisingly, the best performance above this transition temperature was obtained in air; it seems that this composite works well as a cathode material. However the sample with 20% CuO, Fig. 8b, presented a similar performance in air and in methane after the reduction in hydrogen, probably the segregation of metallic Cu to the interface between the YSZ electrolyte and the anode material short circuit the cell and for this reason the performance for methane of 20% CuO, Fig. 8b and 60% CuO, Fig. 8c, was similar to that of pure YZTC6 in methane, Fig. 8a, after reduction in hydrogen.

For the samples with NiO, Fig. 8d and e, the behavior was nearly identical for samples with 20 and 60% of NiO and there was an increase in the performance with respect to the YSZTC6 or its CuO composites, with the lowest series and polarization resistances. The CuO composites, however, had the best performance at temperature below 600°C, in hydrogen.

The total conductivity from polarization and diffusion is usually superior for hydrogen than for methane as can be observed in Fig. 9. In air the conductivity is rather low. But at high temperature (700-900°C) the conductivity was similar for all the gas compositions. In samples with 60% CuO, the Arrhenius plots were not so good, because of the difficulties in fitting of the experimental data to the equivalent circuit model, leading to some values with very large errors. The composite with 20% NiO had a better conductivity that the corresponding CuO composite with the same weight composition, and on the other hand, the total conductivity, for 20% NiO, was the same at 500 and 1000°C, in methane.

Surface and cross-sectional SEM micrographs have been obtained to characterize the samples after the measurements, Fig. 10. The sample with 20% CuO had a very good distribution of porosity, but the sample with higher content in CuO formed agglomerates. The surface contact between the anode material and the electrolyte is seen to be better in the sample with 60% in CuO and 60% NiO. But the cermets with NiO had a very bad porosity distribution, for example, the sample with 60% NiO had large cavities.

Conclusions

The (YZTC6 + 60%CuO) composites at 500°C in reducing conditions present the best behavior and it could be interesting to study this material at lower temperature. At this temperature, the conductivity for 60% CuO composites was about five times higher than the conductivity of the corresponding NiO with the same weight composition. For the cermets with 20% in CuO there was a slight improvement in the conductivity at low temperature. Copper cermets produced from reduction of the oxides suffered serious microstructural degradation above 600°C and this provides a major concern for utilisation of Cu-based anodes in SOFCs. Although the series resistance was slightly lower for the Cu cermets than the simple oxides at high temperatures, the polarization resistances were slightly higher, indicating that the change in microstructure due to Cu migration was detrimental to electrode performance. Ni addition reduced the polarization and series resistances at all temperatures; however, the performance was inferior to the widely used Ni/YSZ cermets, probably due to microstructural factors.

Acknowledgments

The authors gratefully acknowledge the research program CICYT-FEDER-1FD-1422-MAT, EPSRC and OSSEP-ESF for financial support.

References

1. A. J. Appleby and F. R. Foulkes, in *Fuel Cell Handbook*, Van Nostrand Reinhold Press, New York (1989).
2. T. Setoguchi, K. Okamoto, K. Eguchi, and H. Arai, *J. Electrochem. Soc.*, **139**, 2875 (1992).
3. B. C. H. Steele, I. Kelly, H. Middleton, and R. Rudkin, *Solid State Ionics*, **28-30**, 1547 (1988).
4. P. V. Hendriksen, in *Solid Oxide Fuel Cells*, V. S. C. Singhal and H. Tagawa, Editors, PV 97-40, p. 1319, The Electrochemical Society Proceedings Series, Pennington, NJ (1997).
5. N. H. Minh, *J. Am. Ceram. Soc.*, **76**, 563 (1993).
6. D. W. Dees, T. D. Claar, T. E. Easler, D. C. Fee, and F. C. Mrazek, *J. Electrochem. Soc.*, **134**, 2141 (1987).
7. T. Tsai, E. Perry, and S. A. Barnett, *J. Electrochem. Soc.*, **145**, 1696 (1998).
8. J. T. S. Irvine, D. P. Fagg, J. Labrincha, and F. M. B. Marques, *Catal. Today*, **38**, 467 (1997).
9. S. S. Liou and W. L. Worrell, *Appl. Phys. A: Solids Surf.* **49**, 25 (1989).
10. B. Càles and J. F. Baumard, *J. Electrochem. Soc.*, **131**, 2407 (1983).
11. P. V. Ananthapadmanabhan, N. Venkatramani, V. K. Rohatgi, A. C. Momin, and K. S. Venkateswarlu, *J. Eur. Ceram. Soc.*, **6**, 111 (1990).
12. J. C. C. Abrantes, J. A. Labrincha, F. M. B. Marques, and J. R. Frade, in *Ceramics Today-Tomorrow's Ceramics, Part C*, P. Vincenzini, Editor, p. 2265, Elsevier Science, Amsterdam (1991).
13. R. M. C. Marques, J. R. Frade, and F. M. B. Marques, *Bol. Soc. Esp. Ceram. Vidrio*, **30**, 464 (1991).
14. H. Naito and H. Arashi, *Solid State Ionics*, **53-56**, 436 (1992).
15. M. T. Colomer, J. R. Jurado, R. M. C. Marques, F. M. B. Marques, in *Solid Oxide Fuel Cells*, S. C. Singhal and H. I. Iwahara, Editors, PV 93-94, p. 523, The Electrochemical Society Proceedings Series, Pennington, NJ (1994).
16. T. Lindegaard, C. Clausen and M. Mogensen, in *Proceedings of 14th Riso International Symposium on Materials Science*, F. W. Poulsen, J. J. Bentzen, T. Jacobsen, E. Skou, and M. J. L. Ostergard, Editors, p. 311, Riso National Laboratory, Roskilde, Denmark (1993).
17. R. M. Marques and F. M. B. Marques, and J. R. Frade, *Solid State Ionics*, **73**, 27 (1994).
18. M. T. Colomer, J. R. Jurado, R. M. C. Marques, and F. M. B. Marques, *Mater. Res. Bull.*, **30**, 515 (1995).
19. K. E. Swider and W. L. Worrell, *J. Electrochem. Soc.*, **143**, 3706 (1996).
20. M. T. Colomer, P. Durán, A. Caballero, and J. R. Jurado, *Mater. Sci. Eng.*, **A229**, 114 (1997).
21. A. J. Feighery, J. T. S. Irvine, D. P. Fagg, and A. Kaiser, *J. Solid State Chem.*, **143**, 273 (1999).
22. A. Kaiser, A. J. Feighery and J. T. S. Irvine, in *Solid Oxide Fuel Cells*, M. Dokiya and S. C. Singhal, Editors, PV 99-19, p. 541, The Electrochemical Society Proceedings Series, Pennington, NJ (1999).
23. S. P. Jiang, J. G. Love, and S. P. S. Badwal, in *Electrical Properties of Oxide Materials*, J. Nowotny and C. C. Sorrel, Editors, p. 81, Key Engineering Materials, Trans Tech Publications, Switzerland (1997).